

Data Processing Report

Shipboard Acoustic Doppler Current Profiler (75kHz)

R/V Meteor III cruise MET203

Issue date: November 28, 2024

Contact

Robert Kopte (robert.kopte@ifg.uni-kiel.de)

Christian-Albrechts-Universität zu Kiel - Institute of Geosciences

German Marine Research Alliance (DAM) - Underway Research Data Project
datamanagement@marine-data.de

1 Abstract

Current velocities of the upper water column along the cruise track of R/V Meteor III cruise MET203 were collected by a vessel-mounted 75 kHz RDI Ocean Surveyor ADCP.

The ADCP transducer was located at 5.0 m below the water line. The instrument was operated in narrowband mode (WM10) with a bin size of 8.00 m, a blanking distance of 4.00 m, and a total of 100 bins, covering the depth range between 17.0 m and 809.0 m.

Attitude data from the ship's motion reference unit were used by the data acquisition software VmDAS internally to convert ADCP beam velocities to geographic coordinates.

The Python toolbox OSADCP (version 2.0.0) was used for data post-processing. Single-ping data were screened for bottom signals and, where appropriate, a bottom mask was manually processed. Acoustic Interferences were identified based on outliers in the ADCP echo intensity data. Echo intensity data were cleaned accordingly and affected velocity cells were flagged to be removed prior ensemble-averaging.

The ship's velocity was calculated from position fixes obtained by the Global Navigation Satellite System (GNSS), taking into account lever arms of ADCP transducer and GNSS antenna. Accuracy of the derived water velocities mainly depends on the quality of the position fixes and the ship's heading data. Further errors stem from a misalignment of the transducer with the ship's centerline.

Data processing included water track calibration of the misalignment angle ($-46.4281^\circ \pm 0.5612^\circ$) and scale factor (1.0069 ± 0.0086) of the measured velocities. The velocity data were averaged in time using an average interval of 60 s.

Depth cells with ensemble-averaged percent-good values below 25% are marked as 'bad data'.

2 Sensor, configuration and deployment information

Sensor details	
Device	RDI Ocean Surveyor
Frequency	75 kHz
Transducer S/N*	2175-G
Sensor URN	https://hdl.handle.net/10013/sensor.f9164d82-518b-447b-bc75-a8d162edf99a
Transducer depth	5.0 m
Configuration details	
Operating mode	narrowband mode (WM10)
Number of cells	100
Bin length	8.0 m
Blanking distance	4.0 m
Pulse length	8.0 m
Lag	1.46 s
Heading alignment	46.00°
Heading bias	0.00°
Deployment details	
Start Time	2024-08-19T12:23:00Z
End Time	2024-09-24T01:22:00Z
Minimum latitude	4.65°N
Maximum latitude	15.17°N
Minimum longitude	-59.42°E
Maximum longitude	-22.48°E
Minimum depth	17.00 m
Maximum depth	809.00 m
ADCP/GNSS positions*	
ADCP_x	-1.92 m
ADCP_y	26.76 m
GNSS_x	0.00 m
GNSS_y	0.00 m

* Position of ADCP and GNSS antenna relative to the midship position. x positive/negative refers to starboard/portside and y positive/negative refers to ship's bow/ship's deck, respectively. A geometric compensation is applied to account for the different relative positions of transducer and GNSS.

3 Details

3.1 Data acquisition

ADCP raw data were acquired using the data acquisition software VmDAS by Teledyne RDI. Time-synchronous position and attitude data were provided by Kongsberg Seapath systems and added to the ADCP data stream within VmDAS. All data are provided as single-ping ensembles in binary pd0 format (see below).

3.2 Data processing

3.2.1 Processing software

For data processing, the Python-based software OSADCP (version 2.0.0) was used. It is specifically developed both for the near-real-time monitoring and for the delayed-mode processing of shipboard ADCP raw data (Kopte et al., 2024). OSADCP contains modules that include the essential processing steps of coordinate transformation, position data verification, velocity data cleaning, bottom interference detection, ensemble averaging, water-track calibration or bottom-track processing.

For the here described data set, the following OSADCP modules were employed:

- os_settings
- os_read_enx
- os_edit_bottom
- os_backscatter
- os_watertrack

3.2.2 Raw data conversion

VmDAS generates three raw data formats each representing a different status of internally applied coordinate transformation and data stream merging. For the here described data set, ENX files were used for processing, which contain raw velocity data in geographic coordinates and navigation data for each ping.

The binary raw data was converted and arranged in a data structure containing both measured parameters at single-ping level and meta data. Data are checked for completeness and clock drift of the sensor PC. Navigation data are verified and checked for common problems such as the occurrence of zero/zero positions, irregularities in the time allocation such as time stops, backward time jumps, time shifts etc. Affected pings are flagged accordingly and ignored in further processing.

3.2.3 Bottom interference

ADCP single ping data were scanned for echo feedback from the ground, which introduces spurious velocities in the affected cell range. The scanning was carried out based on inspection of the time series of the echo intensity and along-track velocity profiles to identify the bottom signal and its potential effect on the velocities near the sea bed by sidelobe interference. A line corresponding to the depth of bottom influence on the measured velocities was picked manually that was used to exclude these prior to further processing.

3.2.4 Cleaning of echo intensity data

Light acoustic interference below 40 m was removed by flagging spikes in the echo intensity data. For the identification of spikes, an echo intensity anomaly field was created by subtracting the median echo intensity profile from each intensity profile at single-ping level. Cells potentially affected by interference were determined by identifying ping-to-ping differences that either exceed or fall below ± 0.7 of the total standard deviation of ping-to-ping differences. The candidate cells were then checked if they are of single-ping duration and whether the associated intensity spikes extend over several depth cells. All cells that were identified as being affected by acoustic interference were excluded from further processing of both the velocity and echo intensity data.

For the here described data set, stronger acoustic interference was detected that required additional, more vigorous cleaning. From the distribution of the total echo intensity anomaly field, that was additionally median-filtered in time, the first and third quartile were calculated to determine the interquartile range $IQR = Q_3 - Q_1$. The heavy tails at the upper and lower ends of the distribution were then determined by $Q_3 + 0.75 \cdot IQR$ and $Q_1 - 0.75 \cdot IQR$. Values that exceed or fall below the right-sided or left-sided heavy tail were classified as outliers and were additionally excluded from further processing.

3.2.5 Water-track calibration

The ship speed was calculated based on GNSS position data taking into account lever arm information for the given setup of ADCP and GNSS sensor, ignoring pings with questionable navigation data.

A number of automated cleaning criteria were applied to the single-ping velocity data (Kopte et al., 2024).

Subsequently, single-ping data along the water column were averaged into so-called ensembles, with the velocities being vector-averaged. Using ensemble averages reduces the spread of single-ping current estimates, increasing the precision of the measurement. For the here described data set, the chosen average interval was 60.0 seconds.

Water-track calibration was applied to the ensemble-average data. It addresses two different errors (Joyce, 1989; Firing and Hummon, 2010):

- Misalignment error: A deviation of the transducer alignment with respect to the heading reference of the ship introduces a bias with its main effect being a spurious cross-track component proportional to ship speed.
- Scaling error: Small errors in the beam geometry or a non-zero trim of the transducer or ship can cause a systematic bias affecting mostly the along-track velocity component, proportional to ship speed.

The applied algorithm of the water-track calibration is described in detail in Kopte et al., 2024.

Calibration results are documented in Figure 1. The final calibration values α and β were applied to the measured velocities. Subsequently, the ship velocity was subtracted to obtain horizontal water velocities.

	Mean value	Standard deviation
Misalignment angle	-0.4281°	0.5612°
Scale factor	1.0069	0.0086

MISALIGNMENT ANGLE DETERMINATION

2024/11/21 14:30:28

From: 2024/08/19 12:41
To: 2024/09/22 15:36

Total Duration: 34.12 days
Calibration Points: 194599 of 202290

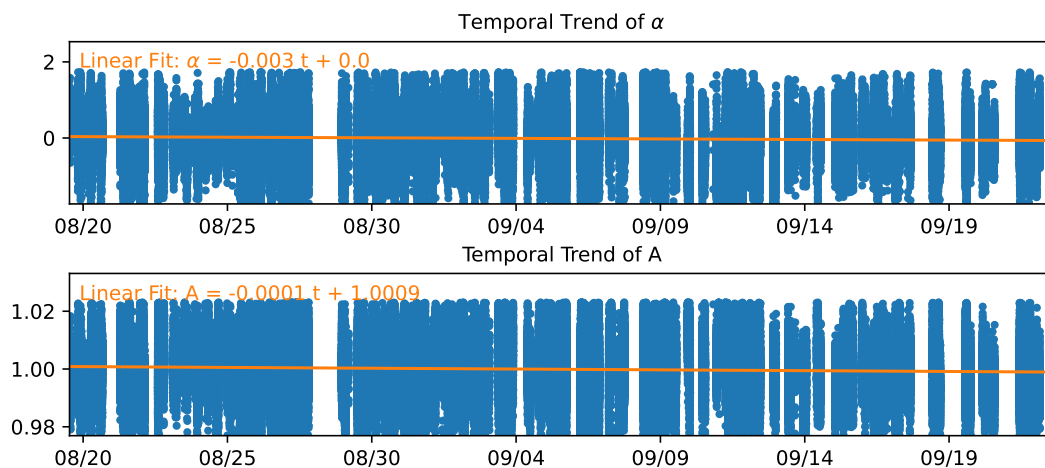
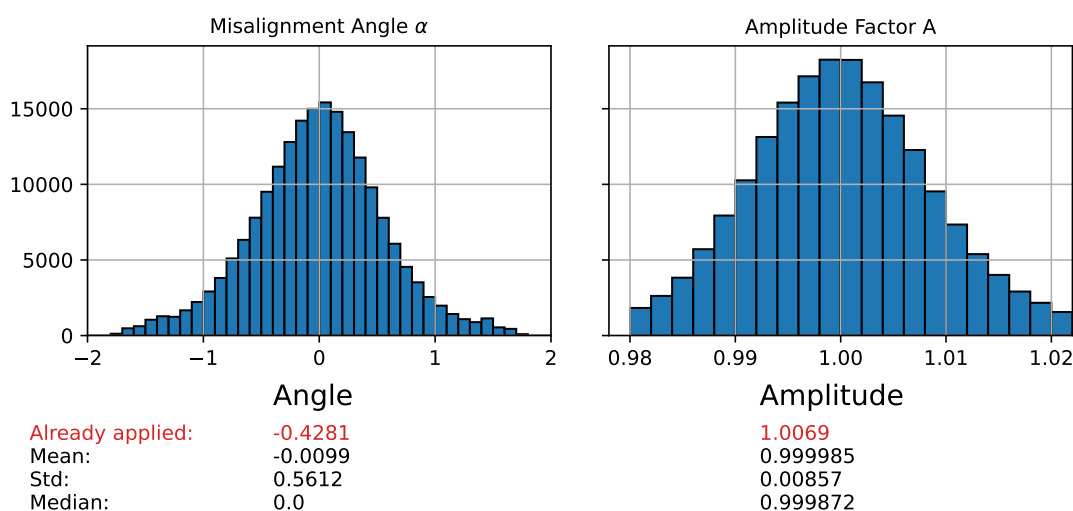


Figure 1: Top: Histograms showing results from misalignment angle (left) and scale factor (right) determination. Bottom: Temporal trend of misalignment angle (upper panel) and scale factor (lower panel).

3.2.6 Calculation of relative backscatter from ADCP echo intensity

Relative acoustic backscatter was calculated from the cleaned echo intensity data by applying a working version of the sonar equation (Mullison, 2017):

$$S_v = C + 10 \log_{10} ((T_x + 273.16)R^2) - L_{DBM} - P_{DBW} + 2\alpha R + 10 \log_{10} (10^{k_c(E-E_r)/10} - 1)$$

where S_v is the relative backscatter, C is a constant combining several parameters specific to each instrument, T_x is the temperature measured at the transducer ($^{\circ}\text{C}$), L_{DBM} is the $10 \log_{10}$ of the transmit pulse length (m), P_{DBW} is the $10 \log_{10}$ of the transmit power (W), R is the along-beam range to scatterers (m), α is the absorption coefficient of water (dB/m), k_c is the conversion factor for echo intensity (dB/counts), E is the measured echo intensity (RSSI, counts), and E_r is the measured echo intensity (RSSI, counts) in the absence of any signal (noise).

In this calculation, the noise floor E_r was neglected, hence the term 'relative backscatter'.

For the RDI Ocean Surveyor 75 kHz system used for this data set, $C = -164.26$ and $P_{DBW} = 24.0$ dB (Mullison, 2017).

The conversion factor k_c was calculated as follows:

$$k_c = \frac{127.3}{(T_x + 273.16)}$$

The slant range R was calculated as follows:

$$R = \left(\frac{B + |P - CS|/2 + (N \cdot CS) + CS/4}{\cos \theta} \right) \left(\frac{c'}{c_x} \right)$$

where B is the blanking distance, P is the pulse length, CS is the cell size, N is the number of cells, θ is the beam angle, c' is the mean sound speed between the transducer depth and the depth of the cell, and c_x is the sound speed at the transducer.

The absorption coefficient of water was calculated as the sum of contributions from boric acid, magnesium sulfate and pure water, following Francois and Garrison (1982). The calculation requires fields of temperature, salinity and sound speed on the ADCP cell grid. The temperature and salinity fields were extracted from the seasonal means over the 2015-2022 period on a $1^{\circ} \times 1^{\circ}$ grid provided by the World Ocean Atlas 2023 Data (Locarnini et al., 2023 and Reagan et al., 2023). The gridded data was interpolated on the ADCP grid along the cruise track. From the interpolated fields, sound velocity was calculated.

3.2.7 Quality control and flags

The flagging scheme follows the SeaDataNet vocabulary for measured qualifier flags (SeaDataNet, 2022; see Figure 2). The central criterion for the quality assessment is the evaluation of the ensemble percent-good value. It is a measure of the number of valid measurements contained in an ensemble-mean. For the here described data set, cells with an ensemble percent-good value below 25% were flagged as 'bad data'.

3.2.8 Meta data standards

The final data product of processed and quality-controlled shipboard ADCP velocity measurements is created as netCDF file (Unidata, 2021).

Meta data standards follow Climate and Forecast conventions (CF-1.6, v19), OceanSites Manual-1.3, EGO glider user manual 1.3, and Attribute Convention for Data Discovery 1.3 (ACDD-1.3). Additionally, all relevant meta information

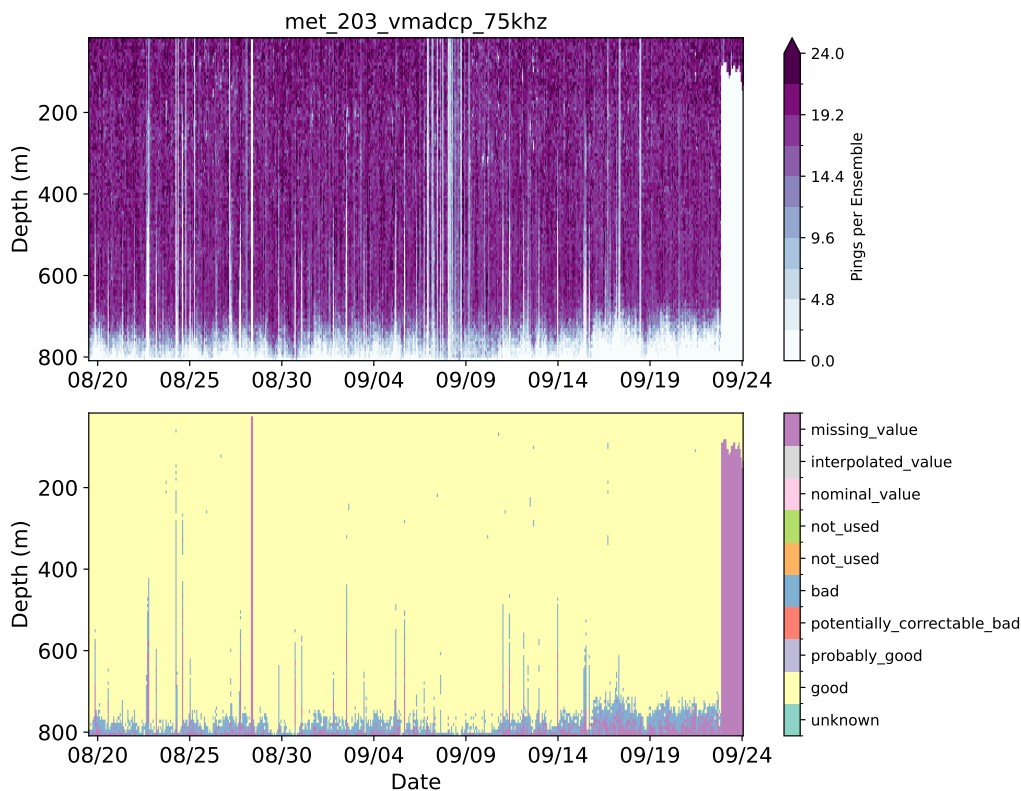


Figure 2: Top: Number of pings used for an ensemble for each cell. Bottom: Distribution of quality flags.

about the deployment, ADCP system, data acquisition and processing parameters are stored as global attributes. The standard name vocabulary to identify data variables is from CF-1.6, v19. Ensemble-mean time series of horizontal velocity profiles and corresponding quality flags are stored as 2-D arrays, as is the ensemble-mean time series of cleaned echo intensity profiles. Time, position, and cell depth information are saved as 1-D vectors.

ADCP data coverage

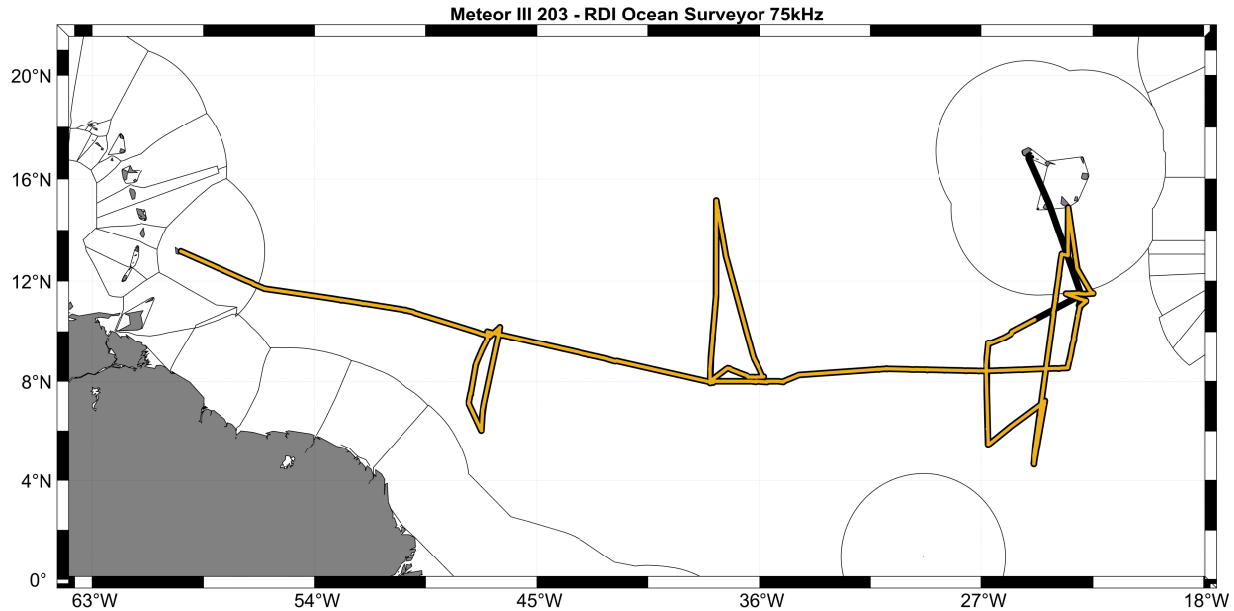


Figure 3: ADCP measurements (orange dots as indicated) along cruise track (black line). EEZs are marked by grey lines.

References

- Firing, E and Hummon, J (2010). Ship-mounted acoustic Doppler current profilers in The GO-SHIP Repeat Manual: A Collection of Expert Reports and Guidelines. Available online at: <http://www.go-ship.org/HydroMan.html>
- Francois, R and Garrison, G (1982). Sound absorption based on ocean measurements: Part II: Boric acid contribution and equation for total absorption. *Journal of the Acoustical Society of America*, 72(6), 1879-1890.
- Joyce, T M (1989). On in situ "Calibration" of shipboard ADCPs. *J. Atmos. Oceanic Technol.* 6, 169-172.
doi: 10.1175/1520-0426(1989)006%3C0169:OISOSA%3E2.0.CO;2
- Kopte R, Becker M, Fischer T, Brandt P, Krahmann G, Betz M, Faber C, Winter C, Karstensen J and Wiemer G (2024). FAIR ADCP data with OS-ADCP: a workflow to process ocean current data from vessel-mounted ADCPs. *Front. Mar. Sci.* 11:1425086. doi: 10.3389/fmars.2024.1425086
- Kopte, R, Betz, M and Anselm, N (2022). SOP 75kHz ADCP aboard of RV Meteor III. Zenodo. <https://doi.org/10.5281/zenodo.7022755>
- Locarnini R A, Mishonov A V, Baranova O K, Reagan J R, Boyer T P, Seidov D, Wang Z, Garcia H E, Bouchard C, Cross S L, Paver C R and Dukhovskoy D (2023). *World Ocean Atlas 2023, Volume 1: Temperature*. A Mishonov Technical Ed. NOAA Atlas NESDIS 89, doi.org/10.25923/54bh-1613
- Mullison (2017). Backscatter Estimation Using Broadband Acoustic Doppler Current Profilers - Updated. Conference paper at 'ASCE Hydraulic Measurements & Experimental Methods Conference', Durham, NH, July 9-12, 2017.
- Reagan J R, Seidov D, Wang Z, Dukhovskoy D, Boyer T P, Locarnini R A, Baranova O K, Mishonov A V, Garcia H E, Bouchard C, Cross S L, and Paver C R (2023). *World Ocean Atlas 2023, Volume 2: Salinity*. A Mishonov, Technical Editor, NOAA Atlas NESDIS 90, doi.org/10.25923/70qt-9574

SeaDataNet (2022). SeaDataNet Measured Qualifier Flags. Available online at: <https://vocab.nerc.ac.uk/collection/L20/current/>

Unidata (2021). Network Common Data Format (netCDF) version 1.5.8 [software]. Boulder, CO: UCAR/Unidata Program Center.
doi: 10.5065/D6H70CW6

List of ENX files used

m203os75002_000000
m203os75002_000001
m203os75002_000002
m203os75002_000003
m203os75002_000004
m203os75002_000005
m203os75002_000006
m203os75002_000007
m203os75002_000008
m203os75002_000009
m203os75002_000010
m203os75002_000011
m203os75002_000012
m203os75002_000013
m203os75002_000014
m203os75002_000015
m203os75002_000016
m203os75002_000017
m203os75002_000018
m203os75002_000019
m203os75002_000020
m203os75002_000021
m203os75002_000022
m203os75002_000023
m203os75002_000024
m203os75002_000025
m203os75002_000026
m203os75002_000027
m203os75002_000028
m203os75002_000029
m203os75002_000030
m203os75002_000031
m203os75002_000032
m203os75002_000033
m203os75002_000034
m203os75002_000035
m203os75002_000036
m203os75002_000037
m203os75002_000038
m203os75002_000039
m203os75002_000040
m203os75002_000041
m203os75002_000042
m203os75002_000043
m203os75002_000044
m203os75002_000045
m203os75002_000046
m203os75002_000047
m203os75002_000048

m203os75002_000049
m203os75002_000050
m203os75002_000051
m203os75002_000052
m203os75002_000053
m203os75002_000054
m203os75002_000055
m203os75002_000056
m203os75002_000057
m203os75002_000058
m203os75002_000059
m203os75002_000060
m203os75002_000061
m203os75002_000062
m203os75002_000063
m203os75002_000064
m203os75002_000065
m203os75002_000066
m203os75002_000067
m203os75002_000068
m203os75002_000069
m203os75002_000070
m203os75002_000071
m203os75002_000072
m203os75002_000073
m203os75002_000074
m203os75002_000075
m203os75002_000076
m203os75002_000077
m203os75002_000078
m203os75002_000079
m203os75002_000080
m203os75002_000081
m203os75002_000082
m203os75002_000083
m203os75002_000084
m203os75002_000085
m203os75002_000086
m203os75002_000087
m203os75002_000088
m203os75002_000089
m203os75002_000090
m203os75002_000091
m203os75002_000092
m203os75002_000093
m203os75002_000094
m203os75002_000095
m203os75002_000096
m203os75002_000097
m203os75002_000098

m203os75002_000099
m203os75002_000100
m203os75002_000101
m203os75002_000102
m203os75002_000103
m203os75002_000104
m203os75002_000105
m203os75002_000106
m203os75002_000107
m203os75002_000108
m203os75002_000109
m203os75002_000110
m203os75002_000111
m203os75002_000112
m203os75002_000113
m203os75002_000114
m203os75002_000115
m203os75002_000116
m203os75002_000117
m203os75002_000118
m203os75002_000119
m203os75002_000120
m203os75002_000121
m203os75002_000122
m203os75002_000123
m203os75002_000124
m203os75002_000125
m203os75002_000126
m203os75002_000127
m203os75002_000128
m203os75002_000129
m203os75002_000130
m203os75002_000131
m203os75002_000132
m203os75002_000133
m203os75002_000134
m203os75002_000135
m203os75002_000136
m203os75002_000137
m203os75002_000138
m203os75002_000139
m203os75002_000140
m203os75002_000141
m203os75002_000142
m203os75002_000143
m203os75002_000144
m203os75002_000145
m203os75002_000146
m203os75002_000147
m203os75002_000148

m203os75002_000149
m203os75002_000150
m203os75002_000151
m203os75002_000152
m203os75002_000153
m203os75002_000154
m203os75002_000155
m203os75002_000156
m203os75002_000157
m203os75002_000158
m203os75002_000159
m203os75002_000160
m203os75002_000161
m203os75002_000162
m203os75002_000163
m203os75002_000164
m203os75002_000165
m203os75002_000166
m203os75002_000167
m203os75002_000168
m203os75002_000169
m203os75002_000170
m203os75002_000171
m203os75002_000172
m203os75002_000173
m203os75002_000174
m203os75002_000175
m203os75002_000176
m203os75002_000177
m203os75002_000178
m203os75002_000179
m203os75002_000180
m203os75002_000181
m203os75002_000182
m203os75002_000183
m203os75002_000184
m203os75002_000185
m203os75002_000186
m203os75002_000187
m203os75002_000188
m203os75002_000189
m203os75002_000190
m203os75002_000191
m203os75002_000192
m203os75002_000193
m203os75002_000194
m203os75002_000195
m203os75002_000196
m203os75002_000197
m203os75002_000198

m203os75002_000199
m203os75002_000200
m203os75002_000201
m203os75002_000202
m203os75002_000203
m203os75002_000204
m203os75002_000205
m203os75002_000206
m203os75002_000207
m203os75002_000208
m203os75002_000209
m203os75002_000210
m203os75002_000211
m203os75002_000212
m203os75002_000213
m203os75002_000214
m203os75002_000215
m203os75002_000216
m203os75002_000217
m203os75002_000218
m203os75002_000219
m203os75002_000220
m203os75002_000221
m203os75002_000222
m203os75002_000223
m203os75002_000224
m203os75002_000225
m203os75002_000226
m203os75002_000227
m203os75002_000228
m203os75002_000229
m203os75002_000230
m203os75002_000231
m203os75002_000232
m203os75002_000233
m203os75002_000234
m203os75002_000235
m203os75002_000236
m203os75002_000237
m203os75002_000238
m203os75002_000239
m203os75002_000240
m203os75002_000241
m203os75002_000242
m203os75002_000243
m203os75002_000244
m203os75002_000245
m203os75002_000246
m203os75002_000247
m203os75002_000248

m203os75002_000249
m203os75002_000250
m203os75002_000251
m203os75002_000252
m203os75002_000253
m203os75002_000254